

Barrier Tunneling and Reflection in the Time and Energy Domains: The Battle of the Exponentials

N. T. Maitra and E. J. Heller

Department of Physics and Harvard-Smithsonian Center for Astrophysics, Harvard University, Cambridge, Massachusetts 02138
(Received 24 January 1997)

The issue of quantum barrier crossing and reflection in the time domain is addressed. We find that (1) classically forbidden barrier tunneling and above-barrier reflection are well-defined and important processes in the time domain, (2) classically forbidden processes can overshadow allowed ones when both are present, and (3) classically allowed trajectories in the time domain are not, in general, sufficient to explain tunneling amplitudes in the energy domain. We also make clear the essential distinction of barriers which flatten out at large distance and those which do not. [S0031-9007(97)03010-X]

PACS numbers: 03.65.Sq, 31.15.Kb

Tunneling through (or reflection from) a barrier at fixed energy E is well understood from a semiclassical (WKB) perspective. WKB theory involves the use of complex trajectories which travel partly in imaginary time in order to penetrate the barrier. The same barrier problems in the time domain have received much less scrutiny, and have caused confusion at times, due to some subtleties which we expose here. For example: *is* there any tunneling in the time domain across a barrier, since classical trajectories can always be found which connect two positions, one on each side of the barrier? The probability amplitude for a particle initially at x_1 to be found at x_2 after time T is given semiclassically by the propagator,

$$G^{\text{sc}}(x_2, T; x_1, 0) = \sum_{\text{cl-paths}} \frac{1}{\sqrt{2\pi i\hbar}} \sqrt{V} e^{(i/\hbar)S_{\text{cl}} - i\nu\pi/2}, \quad (1)$$

which is the classical limit of Feynman's path integral [1]. The sum goes over all classical paths linking x_1 to x_2 in time T , and $S_{\text{cl}} = S_{\text{cl}}(x_2, x_1, T) = \int_{x_1}^{x_2} p_{\text{cl}}(x)dx - E_{\text{cl}}T$ is the action along that path. $p_{\text{cl}}(x) = \sqrt{2m[E_{\text{cl}} - V(x)]}$ is the classical momentum at x of a particle with energy E_{cl} , and E_{cl} is determined by the classical relation $T = m \int_{x_1}^{x_2} dx/p_{\text{cl}}(x)$. V is the Van Vleck determinant $|\partial^2 S_{\text{cl}}/\partial x_2 \partial x_1|$ and ν is the Maslov index. Consider a transmission problem where x_1 and x_2 are on the left and right sides, respectively, of a barrier in an otherwise constant potential. At any real time T there is exactly one classical path with $E_{\text{cl}} > V_{\text{max}}$ which contributes in (1). So the barrier problem in the time domain seemingly does not involve "tunneling" or classically forbidden paths. In order to obtain the semiclassical energy domain Green function, one performs the Fourier transform by stationary phase:

$$G^{\text{sc}}(x_2, x_1; E) = \frac{1}{i\hbar} \int_{sp} e^{iET/\hbar} G^{\text{sc}}(x_2, T; x_1, 0) dT. \quad (2)$$

However, for energies below the barrier top, no real-time stationary phase point is found, forcing a search in the complex-time plane for a saddle point. The search is re-

warded with the well-known classically forbidden imaginary time tunneling trajectories, which asymptotically give the correct WKB fixed energy tunneling amplitudes (transmission $\sim e^{-\int_{a_1}^{a_2} |p_{\text{cl}}| dx/\hbar}$, where $a_{1,2}$ are the classical turning points at energy E). Suppose the semiclassical time domain Green function is very accurate. Then a correspondingly accurate energy domain result would follow from *numerical* Fourier transform and would be different numerically from stationary phase evaluation. It is thus tempting to think that if the original (real-time) Fourier transform over the semiclassical propagator were performed *numerically* (rather than by stationary phase) one would get an even better result. Strangely, such a result would be given only in terms of classically allowed over-the-barrier trajectories [since $G^{\text{sc}}(x_2, T; x_1, 0)$ is]. The smallness of the tunneling amplitude in this view would be due to the rapid oscillation of the integrand. This method was considered in recent work [2]. It is reinforced by analogy with certain *uniformizations* in semiclassical theory, in which troublesome semiclassical amplitudes are replaced by more accurate, "uniform" ones, which can come from an integral expression. The foundation of such an idea was, however, called into doubt in [3], and the situation remained cloudy. Here, we show that the numerical time-energy Fourier integral, using above-barrier information, is indeed inadequate. In fact, below-barrier tunneling trajectories are needed *even in the time domain* in certain regimes, where for finite \hbar they *dominate* the classically allowed result. Moreover, they dominate the Fourier transform at below-barrier energies.

The Time Domain.—The semiclassical recipe (1) for the time Green function calls only for ordinary real-time classical paths linking x_1 to x_2 in time T . For definiteness, we consider a quasiclassical phase space view of propagation across a symmetric Eckart barrier $V_0 \text{sech}^2 x$ and take mass 1. A state $|x\rangle$ may be represented by a vertical line through x corresponding to momentum being completely unspecified when the position is exactly known. Since $\langle x_2 | x_1(t) \rangle = \langle x_2 | e^{-iHt/\hbar} | x_1 \rangle = \langle x_2 | (e^{iHt/2\hbar})^\dagger e^{-iHt/2\hbar} | x_1 \rangle = \langle x_2(-t/2) | x_1(t/2) \rangle$, we may

represent the propagator by the overlap of the phase space distribution from a vertical line at x_1 evolved for time $T/2$ with that of a vertical line at x_2 evolved backward in time for $T/2$. In Fig. 1 we focus on the case $x_1 = -x_2 < 0$ and $V_0 = 1$. We have shown the phase space distribution at four successive times. At first, this distribution simply shears, as it would for free particle motion. Only very high energy trajectories reach the interaction region. As time evolves, lower energy trajectories arrive near the barrier. The classical overlap of the forward and backward propagated distributions is proportional to the Van Vleck determinant. Because of the separatrix and the concomitant exponential instability, the density of trajectories at the intersection $x = 0$ (classically allowed above-barrier trajectories) falls away exponentially rapidly. In the plots, we have propagated a finite uniform density of several hundred trajectories along the initial line; after some time ($t = 10$), the density at the separatrix is so low that the manifold is not seen at $x = 0$. We call this contribution to the time Green function the *A* term (classically allowed, over the barrier). At the same time, however, we see a below-barrier loop structure developing with a healthy density. At time $t = 10$, for example, trajectories of a certain energy (below V_0) have just reached the barrier and are beginning to turn around. The loops are strongly suggestive of a tunneling contribution to the propagator, since they are very similar to the fixed energy manifolds (Fig. 2) which tunnel across the barrier in the energy domain. The loops from x_1 and x_2 make no contribution in the primitive semiclassical limit as they do not overlap. However, if we include *tunneling* between these loops, we have a second contribution to the time Green function, term *B*. For finite, fixed \hbar , a “battle of the exponentials” ensues. The classical term *A* Van Vleck prefactor, which dies exponentially in time, is pitted against the tunneling term *B*, which is a factor bounded by a fixed exponential multiplied by an algebraically decaying prefactor. Thus

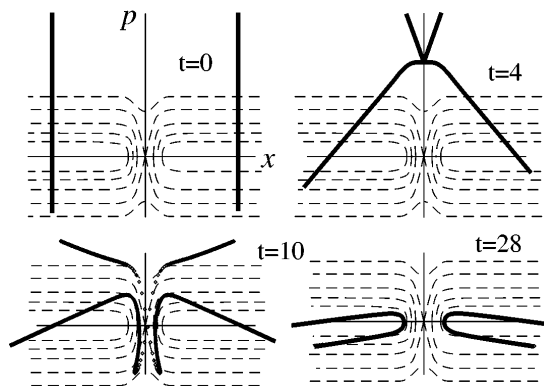


FIG. 1. A quasiclassical view of the propagator $G(10, T; -10, 0)$ in phase space ($t = T/2$) (see text). As time evolves, the density dies exponentially; only at very dense seeding of initial conditions will the thin manifold be seen. “Tunneling loops” develop. Phase space contours are overlaid.

the battle is always lost by the classical term *A* at long times. For the Eckart barrier and end points far from the interaction region, tunneling overtakes the classical contribution when $e^{-\pi(\omega - 2x/T)/\hbar} / \sqrt{T} > \sqrt{\omega/2} e^{x - \omega T/2}$. The right-hand side of this is the square root of the long-time limit of the Van Vleck determinant (term *A*), which determines the magnitude of the semiclassical propagator and ω is the frequency of the (inverted) oscillator in the harmonic approximation to the barrier top. The left-hand side is the tunneling contribution (term *B*) at long times and far end points. To evaluate this, we observe that in this limit the loops approach energy contours, and so the issue of getting across the barrier region becomes identical to the energy tunneling problem. The energy of trajectories arriving at the barrier changes only slowly with time. Moreover, as time increases, the trajectories arriving from the distant points are of lower and lower energy, so the loop “falls through” successively lower energies as time increases. The tunneling part of the amplitude at a given time then follows from the usual energy tunneling at the energy of the arriving trajectories, suitably weighted by their number density. We use expression (1) but substitute the (time-dependent) energy of the loop for the classical energy. This gives the left-hand side of the above inequality: The density on the loops falls off as $1/T$, much slower than the exponential falloff of the classical contribution. Once we have reached the crossover time, *tunneling dominates the classically allowed contribution*. Indeed, the conventional semiclassical propagator using only above-barrier trajectories becomes a much worse approximation at longer times. This is seen in Fig. 3, which shows the exact Green function and the “primitive” semiclassical result, which collapses near $T = 50$. Also shown is the “loop” contribution, which does an excellent job representing the full Green function at such long times. The exact propagator was obtained by numerical Fourier transform of the exact energy Green function for the Eckart barrier; the latter was calculated in [4]. In Figs. 3 and 5, $\hbar = 1$.

Inverted Harmonic Oscillator.—In Ref. [5], Wigner functions are used to show that tunneling at energies below the inverted harmonic oscillator arises through real trajectories with above-barrier energies. However, an

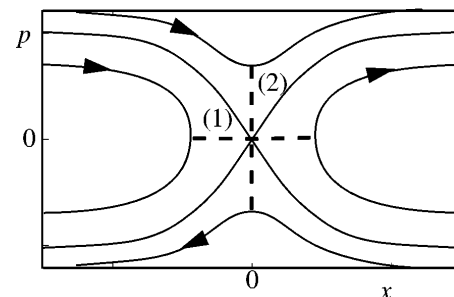


FIG. 2. The classically forbidden processes of tunneling through a barrier (1) and above-barrier reflection (2).

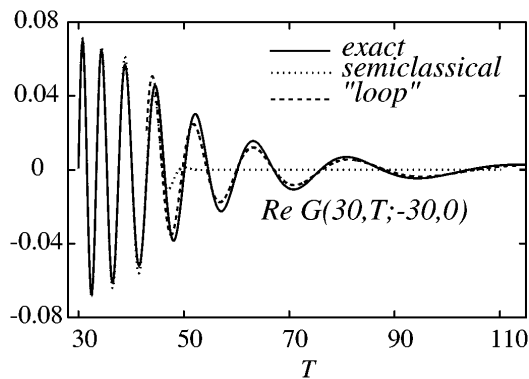


FIG. 3. Transmission through $V = \text{sech}^2 x$: $G(30, T; -30, 0)$.

essential physical aspect of the barrier problem is that it asymptotes to a flat potential, a property which the inverse harmonic potential does not share. This has profound analytic consequences, introducing a branch structure of trajectories in the complex plane [6,7]. In the inverted harmonic case, no tunneling loops develop, since a vertical line at $x = x_1$ representing the initial phase space density always only shears because the dynamics is linear. The conventional semiclassical propagator (which picks up the classically allowed intersection of the forward and backward propagated pieces) is exact in this case. No tunneling trajectories exist to compete with the classically allowed ones. The tunneling loops are also suppressed even for the Eckart-type barriers if $|x_1|, |x_2|$ are near the barrier, where the problem begins to look harmonic. In this limit one might hope the contribution to the semiclassical propagator from the classical “over-the-barrier” overlap would give reasonable results. This was already successfully exploited in [2] and may be of practical significance.

The Energy Domain.—We now consider the probability of tunneling from x_1 to x_2 at energy $E < V_{\max}$. Consider the idea that the classically allowed term is sufficient to use in the numerical transform. The thinking is as follows: The complex-time stationary phase integral (leading to standard WKB results) is an approximation to the Fourier transform over the (primitive) semiclassical propagator (term A); therefore, doing the Fourier transform numerically should yield a better result. However, the first phrase is incorrect: The integral through the complex saddle point is *not* the same integral as the real-time integral. For general end points and barrier potentials, a branch cut in the complex-time plane makes the integral along the complex contour distinct from that along the real-time contour. In fact, in a numerical fast Fourier transform (FFT), *term B must be added to term A as separate contributions to the amplitude*. This is in tune with the essence of the semiclassical limit to Feynman’s path integral, which requires a sum over distinct, stationary paths. The numerical FFT of the semiclassical term A shows a nonphysical end-point dependence at energies below the barrier; as the end points $x_{1,2}$ are moved out beyond the

barrier region, the transmission probability decreases, yet beyond the barrier the motion is free so there must be no amplitude loss [3,7]. The tunneling term B , dominant at long times, is resonant at below-barrier energies, so also dominates the Fourier integral there. One may therefore eliminate the A term when calculating the tunneling, at least in the large $|x_1|, |x_2|$ limit.

The Fourier transform of the B term can be performed by stationary phase; in the large $|x_1|, |x_2|$ limit the result is the usual WKB below-barrier tunneling amplitude which we now show. This is not a contour deformation on the A term; rather, both A and B exist as distinct contributions. When x_1 and x_2 are far from the barrier, the loops approach energy contours of energy $E(T)$, where $E(T) \sim 2x_1^2/T^2$ is the energy needed to arrive at the barrier in time $T/2$. The loop contribution then follows from Eq. (1), where we substitute $E(T)$ in place of the classical energy E_{cl} . The stationary phase point in the time-energy Fourier transform of this at energy E_0 is given by

$$\left. \frac{\partial E}{\partial T} \right|_{T^*} \int_{x_1}^{x_2} \frac{dx}{p_{E(T^*)}} - \left. \frac{\partial E}{\partial T} \right|_{T^*} T^* - E(T^*) + E_0 = 0. \quad (3)$$

Now, by definition, $T = 2 \int_{x_1}^{-x_T} dx/p_{E(T)}(x)$, where $-x_T$ is the (left-hand) turning point at energy $E(T)$. This means the first two terms of Eq. (3) together give

$$-i \int_{-x_T}^{x_T^*} \frac{dx}{|p_{E(T^*)}(x)|} \left. \frac{\partial E}{\partial T} \right|_{T^*} \sim i\pi \frac{\sqrt{2E}}{T^*} = \frac{i\pi E(T)}{|x_1|},$$

where the integral is calculated for the case of the Eckart barrier and we have used the large- x_1 approximation $E(T) \sim 2x_1^2/T^2$ to evaluate the partial derivative. In the large- x_1 limit, this term is ignorable compared to the other two terms of Eq. (3) as it is suppressed by a factor of $1/|x_1|$. The stationary phase condition becomes $E(T^*) = E_0$. This (real) stationary phase point is the time at which a loop of energy E_0 (below the barrier) has formed at time $T/2$, i.e., particles of energy E_0 have just reached their (left-hand) turning point at the barrier in time $T/2$. The prefactor for the stationary phase integral is then calculated from the second derivative of the exponent and, under the large- x_1 approximation, gives $2\pi i \hbar \int_{x_1}^{x_2} dx/p_{E_0(T^*)}^3$. Gathering all factors, we find

$$\int_{sp} G_B e^{iE_0 T/\hbar} dT = \frac{e^{\frac{i}{\hbar} \int_{x_1}^{-x_0} p dx + \frac{i}{\hbar} \int_{x_0}^{x_2} p dx - \frac{1}{\hbar} \int_{-x_0}^{x_0} |p| dx}}{i \hbar \sqrt{p(x_1)p(x_2)}}, \quad (4)$$

which is exactly the WKB result. p, x_0 , etc., are the momentum and turning point at energy E_0 . We note that (4) is also the result of a “FFT” of the classical term A but along the complex-time contour through the saddle point. We stress again that this is not the same integral as the real-time FFT of term A due to the branch cut. We refer the reader to Ref. [7] for a discussion of the branch structure of the primitive semiclassical propagator (term A) in the complex-time plane. Here

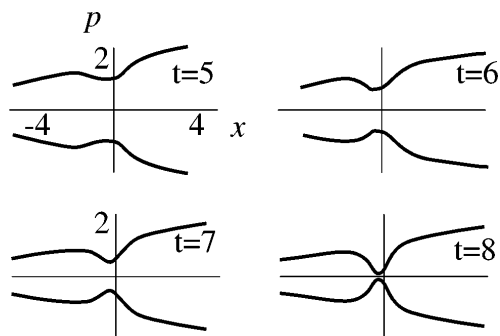


FIG. 4. A quasiclassical view of the propagator $G(-10, T; -10, 0)$ in phase space ($t = T/2$, see text). In this intermediate time range, where there is no classical reflection, contours resembling above-barrier energy contours have formed, suggesting a quantum reflection contribution.

we note that this is different yet closely related to the well-known branch structure of the classical trajectories in the barrier, where branch cuts separate topologically distinct paths differing in the number of passes “under” the barrier [6,7]. This structure leaves its imprint on the classical action $S(x_1, x_2, T)$ and, consequently, on the semiclassical propagator. Whether the branch structure exists is determined by whether singularities of the potential in the complex plane may be reached in finite (complex) time [6,7]. Thus the semiclassical propagator for the harmonic oscillator is entire, but not so for the Eckart barrier. We also suspect (although this is yet to be proven) that the larger $|x_1|, |x_2|$, the more “hidden” is T_A^* behind the branch cut, where T_A^* is the complex time satisfying the stationary phase condition at $E < V_0$ for term A. This happens because of the large real-time propagation outside the barrier region. The contribution from T_A^* is equal to that from the saddle point from term B at the real time $\text{Re}(T_A^*)$, as shown above. This is independent of any real-time contribution from term A (e.g., from a numerical FFT) which vanishes in this limit of far end points. For small $|x_1|, |x_2|$, term B does not exist, and the problem looks harmonic. Indeed, in this case, the complex saddle point from term A is near the branch point, and a permitted contour deformation could pick it up. The distinctness of the A term and integral through the complex saddle point is thus blurred in the small $|x_1|, |x_2|$ limit.

Barrier Reflection.—A similar analysis may also be applied to quantum reflection above a barrier. Taking $x_2 = x_1$ to the left of the barrier in the propagator (1) involves summing over classical paths which have returned after reflection from the barrier as well as the fixed zero-energy trajectory. Clearly, these have energies below the barrier. Until a certain time, real trajectories have not had time to reach the barrier and turn around; only the zero-energy, fixed classical path contributes to the semiclassical amplitude. Quantum above-barrier reflection [process (2) of Fig. 2] plays an important role in this time regime as reflected amplitude interferes with the zero-energy path. In

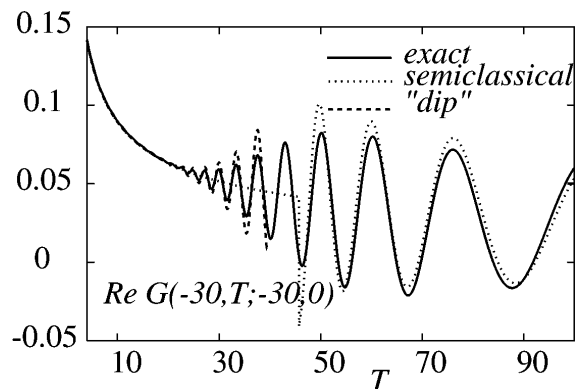


FIG. 5. The reflection propagator $G(-30, T; -30, 0)$.

Fig. 4, we show the quasiclassical picture for reflection where we now take the overlap of the $T/2$ -evolved line from x_1 with its mirror image through the x axis. The latter represents $|x_1(-T/2)\rangle$. We see contours resembling energy contours above the separatrix (Fig. 2), classically disconnected, but across which quantum above-barrier reflection occurs. In analogy to the tunneling case, we may evaluate the quantum reflection contribution at time T , approximating the phase space distribution at an intermediate time by an energy contour at the energy of the trajectory which has reached $x = 0$ at time $T/2$. We then analytically continue the semiclassical reflection propagator to this above-barrier energy, just as in the tunneling loop case. We plot the result in Fig. 5, where our quantum reflection contribution (missing in the primitive semiclassical propagator) well reproduces the oscillations at shorter times.

E. J. H. thanks Bill Miller for energetic discussions over the course of several years, which inspired the present study. N. T. M. thanks Adam Lupu-Sax for help with numerical work, and our whole group for useful discussions. This research was supported by the National Science Foundation under Grant No. CHE-9321260, and through ITAMP at the Harvard-Smithsonian Center for Astrophysics.

- [1] R. Feynman and A. Hibbs, *Quantum Mechanics and Path Integrals* (McGraw-Hill, New York, 1965); B. R. Holstein and A. R. Swift, *Am. J. Phys.* **50**, 829 (1982); R. Rajaraman, *Phys. Rep.* **21C**, 227 (1975); L. S. Schulman, *Techniques and Applications of Path Integration* (Wiley, New York, 1981).
- [2] S. Keshavamurthy and W. H. Miller, *Chem. Phys. Lett.* **218**, 189 (1994).
- [3] F. Grossman and E. J. Heller, *Chem. Phys. Lett.* **241**, 45 (1995).
- [4] H. Kleinert and I. Mustapic, *J. Math. Phys.* **33**, 643 (1992); C. Grosche and F. Steiner, *J. Math. Phys.* **36**, 2354 (1995).
- [5] N. L. Balazs and A. Voros, *Ann. Phys. (N.Y.)* **199**, 123 (1989).
- [6] W. H. Miller, *Adv. Chem. Phys.* **XXV**, 69 (1974).
- [7] N. T. Maitra and E. J. Heller (to be published).